Disabling the folding catalyst is the last critical step in α-lytic protease folding

ERIN L. CUNNINGHAM[1] AND DAVID A. AGARD[2,3]

[1]Graduate Group in Biophysics, [2]Howard Hughes Medical Institute, and [3]Department of Biochemistry and Biophysics, University of California at San Francisco, San Francisco, California 94143-2240, USA

(RECEIVED August 21, 2003; FINAL REVISION October 15, 2003; ACCEPTED October 16, 2003)

Abstract

Alpha-Lytic protease (αLP) is an extracellular bacterial pro-protease marked by extraordinary conformational rigidity and a highly cooperative barrier to unfolding. Although these properties successfully limit its proteolytic destruction, thereby extending the functional lifetime of the protease, they come at the expense of foldability ($t_{1/2}$ = 1800 yr) and thermodynamic stability (native αLP is less stable than the unfolded species). Efficient folding has required the coevolution of a large N-terminal pro region (Pro) that rapidly catalyzes αLP folding ($t_{1/2}$ = 23 sec) and shifts the thermodynamic equilibrium in favor of folded protease through tight native-state binding. Release of active αLP from this stabilizing, but strongly inhibitory, complex requires the proteolytic destruction of Pro. αLP is capable of initiating Pro degradation via cleavage of a flexible loop within the Pro C-terminal domain. This single cleavage event abolishes Pro catalysis while maintaining strong native-state binding. Thus, the loop acts as an Achilles' heel by which the Pro foldase machinery can be safely dismantled, preventing Pro-catalyzed unfolding, without compromising αLP native-state stability. Once the loop is cleaved, Pro is rapidly degraded, releasing active αLP.

Keywords: α-Lytic protease; protein folding; pro region; secondary cleavage; degradation

Secreted by the soil bacterium *Lysobacter enzymogenes*, Alpha-Lytic protease (αLP) is a chymotrypsin-like serine protease (Whitaker 1970; Brayer et al. 1979) that has evolved to resist degradation in harsh, proteolytic environments (Jaswal et al. 2002). αLP achieves a remarkable level of kinetic stability via a large and highly cooperative unfolding barrier of 26 kcal/mole ($t_{1/2}$ = 1.2 yr), which prolongs the functional lifetime of the protease despite the thermodynamic metastability of the αLP native state (Nat) (Sohl et al. 1998; Jaswal et al. 2002; Truhlar et al. 2003). Although this kinetic stability effectively suppresses proteolytic sensitivity, it appears to come at the heavy cost of an extremely high folding barrier (30 kcal/mole; Sohl et al. 1998). Under native conditions, αLP folds to an on-pathway molten-globule intermediate (Int) incapable of converting to the native protease on a biologically feasible timescale ($t_{1/2}$ = 1800 yr). Efficient folding of αLP is only realized in the presence of its requisite Pro (Silen et al. 1989; Baker et al. 1992; Sohl et al. 1998).

Like most extracellular bacterial proteases, αLP is synthesized with a covalent N-terminal pro region extension (Baker et al. 1993). Whether supplied as an attached peptide sequence, as in the naturally occurring protein, or as a separate polypeptide, Pro is essential for the proper folding of αLP (Silen and Agard 1989; Silen et al. 1989). Detailed examination of αLP's Pro-mediated folding mechanism revealed that Pro acts as a folding catalyst, preferentially stabilizing the folding transition state and thereby accelerating the folding rate 3×10^9-fold (Sohl et al. 1998). Recent findings, in combination with earlier studies, indicate a model of Pro-catalyzed folding in which binding of both Pro N- and C-terminal domains serves to arrange key structural elements of the αLP C-terminal domain, allowing the remain-

Reprint requests to: David A. Agard, Howard Hughes Medical Institute and the Department of Biochemistry and Biophysics, University of California at San Francisco, 600 16th Street, Room S412, San Francisco, CA 94143-2240, USA; e-mail: agard@msg.ucsf.edu; fax: (415) 476-1902.

Abbreviations: αLP, α-lytic protease; Pro, wild-type pro region; Int, the intermediate state of αLP; Nat, the native state of αLP; Pro·Nat, complex of Pro with native of αLP; TEV, tobacco etch virus protease; ProTEVloop, Pro with the disordered loop replaced with a TEV protease recognition site; CD, circular dichroism.

Article and publication are at http://www.proteinscience.org/cgi/doi/10.1110/ps.03389704.

der of the αLP N and C domains to dock and fold, thus completing the nascent active site (Peters et al. 1998; Sauter et al. 1998; Cunningham et al. 2002; Cunningham and Agard 2003). Intramolecular processing of the Pro-αLP junction separates the protease from its pro region, with the newly formed αLP N terminus repositioning to its native conformation and the Pro C-terminal tail remaining bound to the active site in an inhibitory manner (Sohl et al. 1997; Sauter et al. 1998). Indeed, Pro maintains a tight association with native αLP, burying >4000 $Å^2$ in the Pro·Nat interface (Sauter et al. 1998). In this way, Pro further promotes αLP folding by driving the thermodynamic equilibrium in favor of the Pro·Nat complex.

As the strongest known inhibitor of αLP (K_i = 0.32 nM), Pro binding greatly stabilizes the folded protease (Peters et al. 1998); however, active αLP must eventually break free of this inhibitory complex in order to fulfill its biological role of degrading other soil microorganisms and providing nutrients to its host. Intermolecular cleavage of secondary cleavage sites within Pro by αLP or other exogenous proteases is presumed to lead to the extracellular destruction of Pro (Sauter et al. 1998; Cunningham et al. 2002). Pro degradation not only releases active αLP, but perhaps more important, it prevents the Pro folding catalyst from accelerating the αLP unfolding reaction as well.

This paper investigates this final, but critical, step of the Pro-catalyzed αLP folding reaction: the necessary destruction of Pro that liberates native, active protease and safeguards αLP from catalyzed unfolding. Here we show that αLP-mediated proteolysis of its Pro folding catalyst occurs via a secondary cleavage event within a disordered loop located in the Pro C-terminal domain. In addition to enabling the rapid destruction of Pro, secondary cleavage in this loop significantly and selectively weakens Pro stabilization of the folding transition state, thus effectively eliminating Pro's ability to catalyze αLP unfolding.

Results

Degradation of Pro by αLP

During the course of Pro-catalyzed αLP folding reactions, the production of active αLP results in Pro degradation. N-terminal sequencing and MALDI mass spectrometry have been used to characterize this proteolysis of Pro. Coomassie-stained SDS-PAGE shows three major Pro degradation bands present in the folding reactions, in addition to the band of uncleaved Pro starting material (Fig. 1). N-terminal sequencing of all four bands revealed the same sequence (PADQV), which corresponds to the N-terminal sequence of Pro, minus the initial methionine that is presumably removed by the host methionine aminopeptidase. The full-length Pro sequence is therefore P2-T168 (sequential numbering), as previously observed in earlier studies of Pro (Sauter et al. 1998).

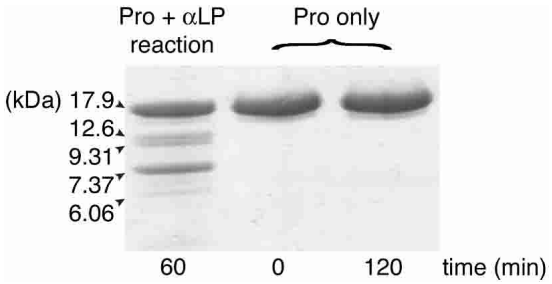

Figure 1. Identification of Pro degradation fragments created by αLP proteolysis. Pro (20 μM) refolds Int (2 μM) to native αLP, which in turn degrades Pro through a series of fragments identified using MALDI mass spectrometry and N-terminal sequencing (Table 1). Initial cleavage occurs within a flexible loop located in the Pro C-terminal domain. Pro alone shows no degradation under the same conditions.

MALDI spectra of the same reactions reveal five unique peaks (Table 1), all with molecular weights equal to or less than full-length Pro (MW = 17,914 Da, P2-T168). The protease (αLP MW = 19.9 kD) was not present in high enough concentrations to be detected. PAWS analysis software was used to identify segments of Pro that are both compatible with the five mass peaks and whose cleavage sites are consistent with the specificity profile of αLP (see Materials and Methods). For the four largest peaks (17.9, 12.6, 9.31, and 7.37 kD), this analysis produces fragment predictions in which P2 is the N-terminal residue, congruent with the N-terminal sequencing data previously discussed (Table 1). The final and smallest mass peak of 6.06 kD matches to four predicted fragments; however, the absence of detectable fragment pairs indicates that the mass peak corresponds to M14-V66, a downstream cleavage product of the 7.37-kD P2-V66 fragment. From these results and from the lack of fragment pairs for the other Pro degradation fragments, it appears that Pro (P2-T168) is first cleaved in a flexible surface loop after residue 117G, then subse-

Table 1. *Pro degradation fragments*

Pro fragment[a]	Calculated mass	Measured mass[b]
P2-T168 (full length)	17,914	17,923 ± 10
P2-G117	12,624	12,642 ± 8.2[c]
P2-V86	9310	9316 ± 1.7
P2-V66	7368	7375 ± 3.5
M14-V66	6058	6065 ± 2.4

[a] N-terminal sequencing was performed on all Pro fragments, except M14-V66.
[b] Average peptide masses (n = 5), measured by MALDI mass spectrometry, are reported with standard deviation errors.
[c] The mass of the P2-G117 fragment appears shifted by ~18 Da, likely due to the binding of a water molecule or a sodium ion.

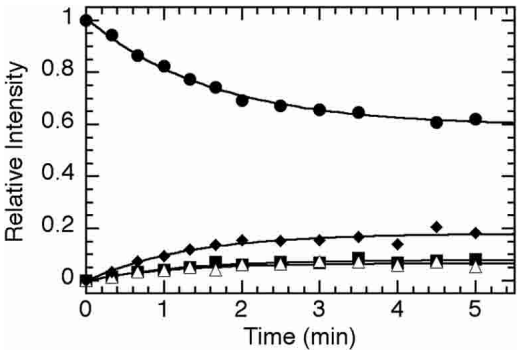

Figure 2. A time course of Pro degradation by αLP. The relative amounts of Pro and Pro fragments created during the catalyzed folding of Int (2 μM) by Pro (20 μM) are shown plotted as a function of time. The cleavage of full-length Pro (circles) occurs at approximately the same rate as the appearance of the 12.6-kD (squares), 9.32-kD (triangles), and 7.37-kD (diamonds) degradation fragments, as determined by single exponential fits of the data (0.63 ± 0.046 min^{-1}, 0.81 ± 0.15 min^{-1}, 0.94 ± 0.26 min^{-1}, and 0.78 ± 0.16 min^{-1}, respectively). Direct addition of native αLP resulted in vastly increased cleavage rates; yet, the extent of Pro degradation was only dependent on the final concentration of native αLP present (data not shown).

quently cleaved after V86 and V66, and finally cleaved before M14.

To further define this putative pathway of successive cleavages, we monitored a time course of Pro degradation during Pro-catalyzed αLP folding by SDS-PAGE. The relative intensities of the resulting gel bands were quantified by gel densitometry and fit with single exponential curves (Fig. 2). This analysis reveals that the cleavage rate of full-length Pro approximately matches the rate of appearance of all of the degradation fragments, with all rates agreeing within experimental error. Varying the initial Pro concentration does not diminish the cooperativity of these proteolytic events; however, it does change the rate at which Int is refolded to active αLP and we find that the observed cleavage rates correlate with the amount of active protease produced (data not shown). Furthermore, degradation experiments in which the absolute and relative concentrations of Pro and Int were varied, or in which native αLP was directly added to Pro, indicate that the extent of proteolysis is solely dependent on the final concentration of native, active αLP (data not shown). Thus, as illustrated by the nonzero plateau of cleaved Pro in Figure 2, although secondary cleavage of the loop enables rapid proteolysis of resultant Pro fragments, it appears that once a critical concentration of degradation products is reached, further proteolysis by αLP is retarded, presumably through either inhibition of the active enzyme or through substrate competition.

Selective cleavage of the Pro disordered loop

Because Pro degradation by αLP is so cooperative, it is not practical to characterize the impact of the initial cleavage event on Pro foldase activity using αLP proteolysis. To circumvent this problem, we replaced the wild-type loop sequence, containing the secondary cleavage site, with the TEV protease (TEV) seven-amino-acid extended recognition site (ProTEVloop). Selective proteolysis using the highly specific TEV allowed us to evaluate the effects of loop cleavage (ProTEVloop$_{cut}$) under conditions that limit the subsequent downstream cleavage events produced by αLP proteolytic activity.

Introduction of the reengineered loop decreases Pro stability, but does not significantly alter Pro function (Table 2). As observed by far UV CD, TEV proteolysis of the loop further destabilizes ProTEVloop, yet structure is restored on binding to native αLP (data not shown). The similarities between the intact and cleaved ProTEVloop·Nat complex CD spectra indicate that although the ProTEVloop$_{cut}$ fragments are no longer covalently attached, they both associate with αLP in the native-state complex in a manner analogous to intact ProTEVloop.

Functional consequences of loop cleavage

The affinities of the ProTEVloop variants for native αLP were measured via their inhibition of αLP activity (Fig. 3). ProTEVloop$_{uncut}$ demonstrates tight-binding inhibition of αLP ($K_i = 0.26 \pm 0.071$ nM) that is within error of the value for wild-type Pro (Table 2). Loop cleavage only slightly weakens native-state binding ($K_i = 1.4 \pm 0.097$ nM), but does shift Pro inhibition from the tight-binding regime to one of simple competitive inhibition.

Although native-state binding appears fairly insensitive to loop cleavage, of central concern is the consequence of loop cleavage on the ability of Pro to catalyze αLP folding.

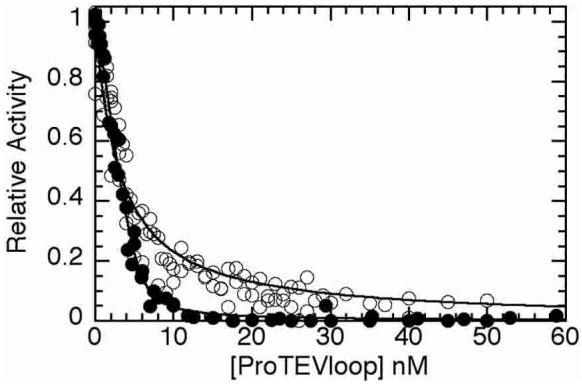

Figure 3. ProTEVloop inhibition of native αLP. Increasing amounts of ProTEVloop$_{uncut}$ (filled circles) and ProTEVloop$_{cut}$ (open circles) reduce the proteolytic activity of 6 nM and 0.25 nM native αLP, respectively. ProTEVloop$_{uncut}$ displays tight-binding inhibition of αLP ($K_i = 0.26 \pm 0.071$ nM) similar to that of wild-type Pro (Table 2). Loop cleavage results in an approximately fourfold loss in affinity for native αLP ($K_i = 1.4 \pm 0.097$ nM), with ProTEVloop$_{cut}$ acting as a simple competitive inhibitor instead of a tight-binding inhibitor.

Table 2. *Stability and function of Pro variants*

Pro variant	$\Delta G_{unfolding}$ (kcal/mole)	K_i (nM)	k_{cat} (min^{-1})	K_M (μM)	Relative k_{cat}/K_M
Wild type	2.0 ± 0.10[a]	0.32[b]	1.9 ± 0.17[c]	24 ± 6.1[c]	1.0
ProTEVloop$_{uncut}$	0.1 ± 0.04	0.26 ± 0.071	1.8 ± 0.32	17 ± 6.3	1.3
ProTEVloop$_{cut}$	<0	1.4 ± 0.097	$\leq 7.7 \times 10^{-7}$	73 ± 13	$\leq 1.3 \times 10^{-7}$

[a] $\Delta G_{unfolding}$ value for wild-type Pro taken from Cunningham et al (2002).
[b] K_i value for wild-type Pro taken from Peters et al. (1998).
[c] Kinetic constants for wild-type Pro taken from Derman and Agard (2000).

Specifically, does secondary cleavage impact either formation of the initial binding (Michaelis) complex with Int (Pro·Int), or the transition state complex, as reflected in K_M and k_{cat} values, respectively? Detailed kinetic analysis of ProTEVloop$_{uncut}$-mediated refolding reactions showed little change in affinity for Int or the folding transition state compared with wild-type Pro (Fig. 4A and Table 2).

In sharp contrast, loop cleavage dramatically reduces catalyzed αLP refolding. As illustrated in Figure 4B, the apparent refolding rate of the ProTEVloop$_{cut}$-assisted reaction is diminished >8000-fold compared with its uncleaved counterpart. Furthermore, analysis of duplicate refolding reactions, which contained different preparations of ProTEVloop$_{cut}$, indicated that the observed acceleration of the αLP refolding rate over that of the uncatalyzed reaction is not dependent on the concentration of ProTEVloop$_{cut}$, but is primarily due to the small amount of residual ProTEVloop$_{uncut}$ present in the refolding reactions (data not shown). Incomplete TEV proteolysis results in trace amounts (<1%) of uncleaved material that can be visualized and quantified by silver-stained SDS-PAGE (data not shown). From these data and by considering the detection limits of the assay conditions, we estimate that loop cleavage significantly reduces ProTEVloop catalysis by at least seven orders of magnitude, such that the observed refolding rates of these reactions are almost completely due to residual ProTEVloop$_{uncut}$ catalyzing the folding of αLP.

Because the extremely slow rate of ProTEVloop$_{cut}$-catalyzed folding is only a minor component of the overall refolding reaction under these conditions, it is impossible to accurately determine K_M and k_{cat} values for the TEV-cleaved variant from a full enzymatic profile as was done for ProTEVloop$_{uncut}$ (see Fig. 4A). Yet, it is mechanistically quite important to discern whether loop cleavage specifically debilitates catalysis (k_{cat}), or greatly weakens initial binding to Int (K_M). Therefore, the effect of loop cleavage on Int binding was measured through the ability of ProTEVloop$_{cut}$ to compete with wild-type Pro-catalyzed αLP refolding. In Figure 4C, we see that addition of ProTEVloop$_{cut}$ to wild-type Pro-catalyzed αLP refolding reactions does not enhance, but instead, slows the initial refolding rate, as ProTEVloop$_{cut}$ appears to effectively compete with wild-type Pro for Int binding, but is then unable to catalyze folding to Nat. Although aggregation of ProTEVloop$_{cut}$ at concentrations higher than 20 μM limits this analysis, a fit of the data to the competitive inhibitor variant of the Michaelis-Menten equation estimates ProTEVloop$_{cut}$ affinity for Int to be ~70 μM (see Table 2). Thus, Pro binding to Int is only weakened approximately fourfold by secondary cleavage, making the apparent $\geq 10^7$-fold ProTEVloop$_{cut}$ folding defect primarily a k_{cat} effect.

Kinetic modeling of ProTEVloop-catalyzed folding

Returning to the ProTEVloop$_{cut}$-catalyzed folding reaction shown in Figure 4B, we now know that αLP folding is catalyzed by trace amounts of ProTEVloop$_{uncut}$ because loop cleavage effectively abolishes ProTEVloop catalysis. Yet, although the observed rate of αLP refolding correlates with the concentration of residual ProTEVloop$_{uncut}$ present in the reaction, neither the refolding rate, nor the amount of αLP refolded, agree with values predicted from the ProTEVloop$_{uncut}$ kinetic constants (see Table 2). Having determined these rate and affinity constants for both ProTEVloop variants, we used these kinetic parameters to model ProTEVloop-catalyzed folding, using the Berkeley Madonna modeling and analysis software (http://www.berkeleymadonna.com), to better understand this anomalous behavior. Comparisons of direct measurements and simulated data from the model (Fig. 5) reveal that, as expected, refolding of Int by substoichiometric quantities of uncut ProTEVloop is dominated by single-turnover kinetics, in which the tight association of the ProTEVloop$_{uncut}$·Nat complex prevents multiple rounds of refolding catalysis. However, when micromolar concentrations of TEV-cleaved ProTEVloop are also present, competition for native αLP binding appears to free intact ProTEVloop$_{uncut}$ to refold multiple Int molecules, consistent with experimental observations. Under these conditions, the αLP refolding rate is not dependent on the rate of ProTEVloop$_{uncut}$ catalysis, but instead on the rate at which ProTEVloop$_{uncut}$ is released from its complex with native αLP.

Discussion

The destruction of Pro is critical to both the release of active αLP and to the prevention of catalyzed αLP unfolding.

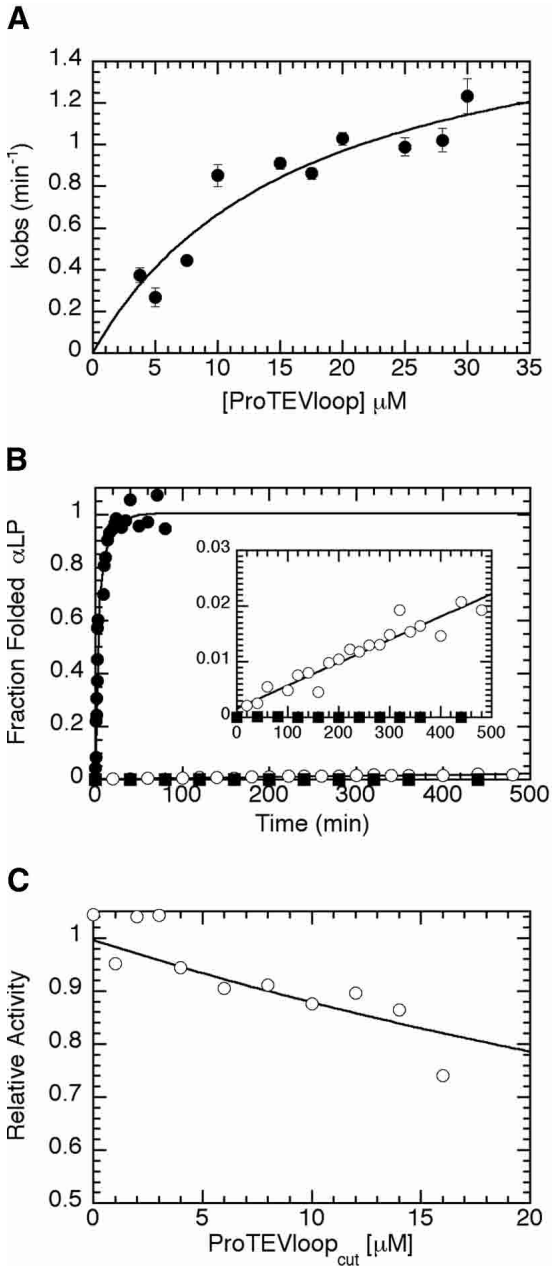

Figure 4. The effect of loop cleavage on the catalyzed folding of αLP. (*A*) A full enzymatic profile of ProTEVloop$_{uncut}$-catalyzed αLP folding, in which catalyzed folding rate constants are plotted as a function of ProTEVloop$_{uncut}$ concentration and the data are fit to a variant of the Michaelis-Menten equation, gives kinetic constants (k_{cat} and K_M) within error of those for wild-type Pro (Table 2). (*B*) The fraction of Int (0.8 μM) refolded to native αLP, both in the absence of catalyst (filled squares) and in the presence of either 3.75 μM intact (filled circles) or TEV-cleaved (open circles) ProTEVloop, is plotted as a function of time. The resulting progress curves illustrate that although ProTEVloop$_{cut}$ accelerates folding ($k_{obs} = 4.2\times10^{-5} \pm 0.29\times10^{-5}$ min^{-1}) over that of the uncatalyzed reaction (*inset*), this rate of refolding is substantially slower than the ProTEVloop$_{uncut}$-catalyzed folding reaction ($k_{obs} = 0.37 \pm 0.036$ min^{-1}). (*C*) The addition of increasing amounts of ProTEVloop$_{cut}$ to wild-type Pro-catalyzed refolding reactions retards initial refolding rates, as ProTEVloop$_{cut}$ competes for Int binding ($K_i = 73 \pm 13$ μM), but cannot catalyze refolding to native αLP (see Table 2).

Although Pro degradation is likely accomplished by a number of exogenous proteases in vivo, αLP is capable of initiating Pro destruction by cleaving a flexible loop within the Pro C-terminal domain. Cleavage of this loop produces Pro fragments that are rapidly degraded by αLP through a series of successive proteolytic events at rates that are kinetically indistinguishable from the rate of initial loop cleavage. The degradation of Pro, like that of many globular proteins, is therefore a cooperative cleavage process: Once the full-length protein is cleaved, it becomes destabilized, making subsequent fragments much more susceptible to further proteolysis (Fontana et al. 1993). Furthermore, whether refolded from Int, or directly added as native protease, αLP only cleaves a fraction of Pro molecules, resulting in a nonzero plateau (Fig. 2) that is dependent on the concentration of αLP, but not Pro, present in the reaction. This finding indicates that Pro bound to native αLP is much more susceptible to cleavage than free Pro, or Pro that is complexed with either Int or the folding transition state. Previous work (Sohl et al. 1997; Cunningham et al. 2002) has shown that differential binding to the transition state and ground state creates significant strain within the Pro·Nat complex. Our data now indicate that this strain promotes secondary loop cleavage, a beneficial mechanism that would favor the destruction of Pro only after αLP folding is complete.

As demonstrated by the kinetic analysis of intact and cleaved ProTEVloop-catalyzed αLP folding reactions, loop cleavage also asserts a dramatic and selective effect on transition-state stabilization. Whereas loop cleavage nearly abolishes stabilization of the folding transition state, the affinity of ProTEVloop$_{cut}$ for either Int or Nat ground states is only reduced approximately fourfold compared with uncleaved ProTEVloop, or WT Pro. This minor reduction in affinity for Int and native αLP likely arises from the instability of ProTEVloop$_{cut}$, as binding energy must be diverted to the restructuring of unfolded ProTEVloop$_{cut}$.

In all previous αLP refolding studies, Pro has behaved as a single-turnover catalyst, with tight native-state binding preventing Pro from being released to fold multiple Int molecules. Interestingly, in refolding reactions containing both forms of ProTEVloop, the strong native-state binding of the catalytically inactive ProTEVloop$_{cut}$ enables it to compete with intact ProTEVloop for binding to native αLP, freeing the potent ProTEVloop$_{uncut}$ catalyst to facilitate multiple rounds of folding. Kinetic modeling of these reactions agrees well with the observed refolding behaviors, which provide the first evidence of multiple turnover in pro region-mediated refolding, further supporting the idea that pro regions function as true folding catalysts.

Most important, differential binding of Pro to the native state versus the folding transition state upon loop cleavage secures the success of the αLP folding reaction despite the thermodynamic instability of the folded product. The single

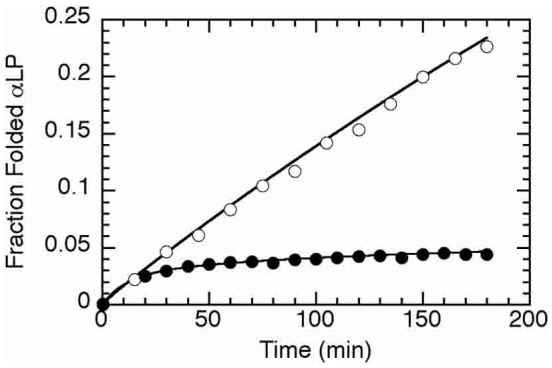

Figure 5. Modeling of ProTEVloop-catalyzed αLP refolding demonstrates multiple turnover. The fraction of Int (0.8 μM) refolded to native αLP by 24 nM ProTEVloop$_{uncut}$, alone (filled circles) and in the presence of 9 μM ProTEVloop$_{cut}$ (open circles), is plotted as a function of time with data generated from kinetic simulations of modeled ProTEVloop-catalyzed folding reactions (solid lines) for both refolding scenarios. The kinetic model is consistent with the observed folding behaviors, including the increase in αLP folding seen on addition of excess, but catalytically inactive, ProTEVloop$_{cut}$. Competition for native αLP binding appears to allow ProTEVloop$_{uncut}$ to catalyze multiple rounds of αLP folding.

cleavage event within the flexible Pro loop effectively disables Pro catalysis while maintaining a strong affinity for the native protease, thereby ensuring native-state stabilization while simultaneously neutralizing Pro's catalytic activity. This highly selective and ordered deactivation of the Pro folding catalyst prevents native αLP from undergoing catalyzed unfolding to the thermodynamically favored Int and unfolded states. Thus, as with many aspects of αLP folding and stability, the mechanism of Pro destruction also appears to be highly optimized. Once Pro is destroyed, the αLP folding pathway is completed, leaving the protease kinetically trapped in its active conformation by a large and extremely cooperative unfolding barrier that imparts αLP with a remarkable resistance to proteolysis.

Materials and methods

ProTEVloop construct

Silent mutations were introduced into the Pro gene (pT7XmaPro plasmid; Sohl et al. 1997) using PCR and QuickChange mutagenesis to create two unique restriction sites, MfeI and SnaBI (pT7XmaProMS). Pro loop residues 107–115 were replaced with the TEV protease recognition sequence (ENLYFQG) by ligating a synthetic oligonucleotide cassette into the pT7XmaProMS plasmid digested with MfeI and SnaBI. All oligonucleotides were synthesized by Invitrogen and mutations were verified by sequencing.

Protein expression and purification

Wild-type Pro and ProTEVloop were purified as described (Derman and Agard 2000), with a portion of wild-type Pro further purified by hydrophobic interaction chromatography (Sauter et al. 1998). Both Pro variants contain an additional N-terminal proline residue, a cloning artifact that does not affect the behavior of Pro (Peters et al. 1998). Wild-type αLP was prepared according to published protocols (Hunkapiller et al. 1973; Mace and Agard 1995) and a portion was denatured as described (Derman and Agard 2000).

Identification and kinetic analysis of Pro degradation fragments

The production of Pro fragments during Pro-catalyzed αLP folding (Sohl et al. 1998) was followed by SDS-PAGE. Protein bands were blotted onto PVDF membrane and visualized by nonacidic Coomassie Brilliant Blue stain, then excised and N-terminally sequenced by Dr. Chris Turck at the Howard Hughes Medical Institute at the University of California at San Francisco. Additional aliquots of the folding reaction were mixed 1 : 1 with 10 mg/mL sinnapinic acid, 60% acetonitrile, and 0.03% TFA and analyzed by MALDI mass spectrometry. Pro fragments with masses that matched the detected mass peaks and that were consistent with αLP's specificity profile (P1 residues in which k_{cat}/K_M >100; G, A, V, T, S, Q, M, C; Mace 1995) were identified using the PAWS freeware edition software version 8.1.1 (ProteoMetrics).

At various time points, aliquots from Pro-catalyzed refolding reactions were removed to reducing SDS sample buffer that was acidified with 1M HCl such that the resultant gel samples were at pH 5, effectively eliminating artifactual proteolysis during sample denaturation. Samples were run on 20% acrylamide Phast Gels (Pharmacia) and Coomassie stained, and the relative intensities of the protein bands were quantified and normalized within each lane using Kodak 1D Image Analysis Software version 3.5.2.

ProTEVloop cleavage by TEV protease

ProTEVloop was incubated with recombinant TEV protease (Invitrogen) at 4°C and 25°C, according to the manufacturer's recommended cleavage conditions, until <1% of ProTEVloop remained uncut, as determined by silver-stained SDS-PAGE with uncleaved ProTEVloop standards. The HIS-tagged TEV protease was removed with Ni-NTA resin and ProTEVloop was exchanged into 20 mM potassium succinate (pH 5.6).

Stability measurements

ProTEVloop$_{uncut}$ stability was analyzed by urea denaturation as described (Cunningham et al. 2002) and in the presence of 15% glycerol to better define the folded baseline. Determination of ProTEVloop$_{cut}$ stability was limited to an upper estimate of $\Delta G < 0$, as the cleaved mutant was unstructured in the absence of urea.

Inhibition measurements

Tight-binding inhibition of 6 nM αLP by ProTEVloop$_{uncut}$ was determined as described (Cunningham et al. 2002). A modified inhibition assay developed for unstable Pro mutants (Cunningham et al. 2002) was used to assess inhibition of 0.25 nM αLP by ProTEVloop$_{cut}$.

ProTEVloop-catalyzed folding

$ProTEVloop_{uncut}$-mediated folding of αLP was performed and analyzed as described (Derman and Agard 2000), except the amplitudes of the biphasic refolding curves were fixed at a consensus ratio of 65 : 35 (fast phase : slow phase).

The catalyzed folding of αLP by $ProTEVloop_{cut}$ was sufficiently slow as to require the use of a very sensitive thiobenzyl ester substrate assay (Sohl et al. 1998; Derman and Agard 2000). Int (1 μM) was incubated alone and in the presence of 2–17.5 μM $ProTEVloop_{cut}$ and αLP refolding was monitored as described (Cunningham et al. 2002). The resultant initial rates of refolding were fit to the linear portion of the exponential refolding curves to determine the k_{obs} magnitude for each refolding reaction.

Initial binding of $ProTEVloop_{cut}$ to Int was determined through competition assays with wild-type Pro in which the initial rate of wild-type Pro-catalyzed αLP refolding was observed in the presence of increasing amounts of $ProTEVloop_{cut}$ and the data were fit to the competitive inhibitor variation of the Michaelis-Menten equation to extract a $K_{i,Int}$ ($\sim K_M$) for $ProTEVloop_{cut}$. For all $ProTEVloop_{cut}$ refolding reactions, the concentration of uncleaved ProTEVloop contaminant was quantified by gel densitometry of silver-stained SDS-PAGE of $ProTEVloop_{cut}$ stocks and $ProTEVloop_{uncut}$ standards.

Data analysis

Data analysis was performed using the Kaleidagraph version 3.08 (Synergy Software) unless otherwise specified. Modeling of ProTEVloop-mediated refolding reactions was done using the Berkeley Madonna version 8.1β5 kinetic simulation software (http://www.berkeleymadonna.com).

Acknowledgments

We thank Dr. Luke Rice and Stephanie Truhlar for many helpful discussions and Peter Chien for his assistance with the PAWS analysis software. This work was supported by the Howard Hughes Medical Institute.

The publication costs of this article were defrayed in part by payment of page charges. This article must therefore be hereby marked "advertisement" in accordance with 18 USC section 1734 solely to indicate this fact.

References

Baker, D., Sohl, J.L., and Agard, D.A. 1992. A protein-folding reaction under kinetic control. *Nature* **356:** 263–265.

Baker, D., Shiau, A.K., and Agard, D.A. 1993. The role of pro regions in protein folding. *Curr. Opin. Cell Biol.* **5:** 966–970.

Brayer, G.D., Delbaere, L.T.J., and James, M.N.G. 1979. Molecular structure of the α-lytic protease from Myxobacter 495 at 2 Å resolution. *J. Mol. Biol.* **131:** 743–775.

Cunningham, E.L. and Agard, D.A. 2003. Interdependent folding of the N- and C-terminal domains defines the cooperative folding of α-lytic protease. *Biochemistry* **42:** 13212–13219.

Cunningham, E.L., Mau, T., Truhlar, S.M.E., and Agard, D.A. 2002. The pro region N-terminal domain provides specific interactions required for catalysis of α-lytic protease folding. *Biochemistry* **41:** 8860–8867.

Derman, A.I. and Agard, D.A. 2000. Two energetically disparate folding pathways of α-lytic protease share a single transition state. *Nat. Struct. Biol.* **7:** 394–397.

Fontana, A., Polverino de Laureto, P., and De Filippis, V. 1993. Molecular aspects of proteolysis of globular proteins. In *Protein stability and stabilization* (eds. W. Van den Tweel et al.), pp. 101–110. Elsevier Science Publications, Amsterdam.

Hunkapiller, M.W., Smallcombe, S.H., Whitaker, D.R., and Richards, J.H. 1973. Carbon nuclear magnetic resonance studies of the histidine residue in α-lytic protease. Implications for the catalytic mechanism of serine proteases. *Biochemistry* **12:** 4732–4743.

Jaswal, S.S., Sohl, J.L., Davis, J.H., and Agard, D.A. 2002. Energetic landscape of α-lytic protease optimizes longevity through kinetic stability. *Nature* **415:** 343–346.

Mace, J.E. 1995. "The 216–226 surface loop of α-lytic protease: Direct and indirect effects on enzyme production, structure and substrate specificity." Ph.D. thesis, University of California, San Francisco.

Mace, J.E. and Agard, D.A. 1995. Kinetic and structural characterization of mutations of glycine 216 in α-lytic protease: A new target for engineering substrate specificity. *J. Mol. Biol.* **254:** 720–736.

Peters, R.J., Shiau, A.K., Sohl, J.L., Anderson, D.E., Tang, G., Silen, J.L., and Agard, D.A. 1998. Pro region C-terminus: Protease active site interactions are critical in catalyzing the folding of α-lytic protease. *Biochemistry* **37:** 12058–12067.

Sauter, N.K., Mau, T., Rader, S.D., and Agard, D.A. 1998. Structure of α-lytic protease complexed with its pro region. *Nat. Struct. Biol.* **5:** 945–950.

Silen, J.L. and Agard, D.A. 1989. The α-lytic protease pro-region does not require a physical linkage to activate the protease domain in vivo. *Nature* **341:** 462–464.

Silen, J.L., Frank, D., Fujishige, A., Bone, R., and Agard, D.A. 1989. Analysis of prepro-α-lytic protease expression in *Escherichia coli* reveals that the pro region is required for activity. *J. Bacteriol.* **171:** 1320–1325.

Sohl, J.L., Shiau, A.K., Rader, S.D., Wilk, B., and Agard, D.A. 1997. Inhibition of α-lytic protease by pro region c-terminal steric occlusion of the active site. *Biochemistry* **36:** 3894–3902.

Sohl, J.L., Jaswal, S.S., and Agard, D.A. 1998. Unfolded conformations of α-lytic protease are more stable than its native state. *Nature* **395:** 817–819.

Truhlar, S.M.E., Cunningham, E.L., and Agard, D.A. 2003. The folding landscape of *Streptomyces griseus* protease B reveals the energetic costs and benefits associated with evolving kinetic stability. *Protein Sci.* (this issue)

Whitaker, D.R. 1970. The α-lytic protease of a myxobacterium. In *Methods in Enzymology,* (eds. G.E. Perlmann and L. Lorand), pp. 599–613. Academic Press, New York.